Electronic Supplementary Material (ESI) for Chemical Communications

Supporting Information for

Morphology and Phase Controlled Cobalt Nanostructures in Magnetic Polypropylene Nanocomposites: Role of Alkyl Chain-Length in Maleic Anhydride Grafted Polypropylene

Qingliang He,[a,b] Tingting Yuan,[a] Zhiping Luo,[c] Neel Haldolaarachchige,[d] David P. Young,[d] Suying Wei[b*] and Zhanhu Guo[a*]

S1.1. Materials

The polypropylene (PP) used in this study was supplied by Total Petrochemicals USA, Inc (ρ=0.9 g/cm^3, M_n≈40500, M_w≈155000, melt index≈35 g/min). Two types of MA-g-PP (provided by Baker Hughes Inc.) were used in these experiments. The first MA-g-PP-1 (M_n≈2500) has a homo-polypropylene with one terminal maleic anhydride (MA) through Alder-ENE reaction. And the second MA-g-PP-2 (M_n≈800) has a propylene-hexene copolymer with one MA group at one terminal and the other MA grafted on the main chain. The structures are shown in Scheme S1. Dicobalt octacarbonyl ($Co_2(CO)_8$, stabilized with 1-5% hexane) was obtained from Strem Chemicals, Inc. Solvent xylene (laboratory grade, ρ=0.87 g/cm^3) was purchased from Fisher Scientific. All the chemicals were used as-received without any further treatment.

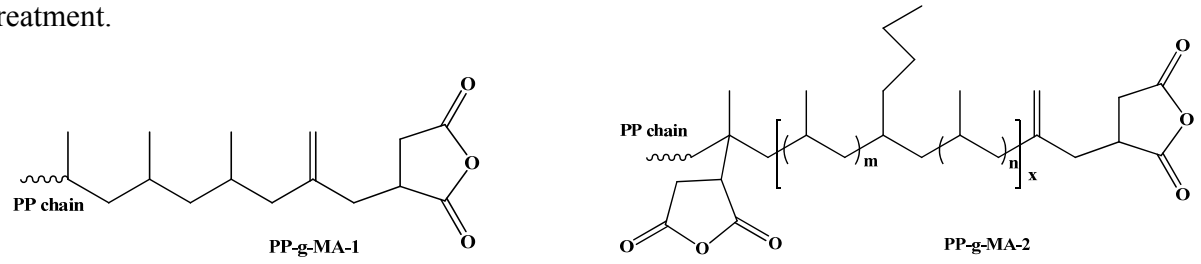

Scheme S1. Chemical structures of MA-g-PP.

S1.2 Preparation of Polymer Nanocomposites

The typical synthesis of PP/Co nanocomposites is summarized as follows. First, 7.5 g PP pellets, 0.5 g MA-g-PP (type 1, or 2) and 100 mL xylene were added into a 500 mL three-neck round bottom flask. Second, the mixture solutions was then heated to the reflux (at 140 °C) under mechanic stirring at 200 rpm, and kept refluxing for 2 hours to fully dissolve PP and MA-g-PP into a homogeneous transparent solution. Third, the solution was cooled down to 110~120 °C; meanwhile, 5.8 g $Co_2(CO)_8$ was dissolved in 120~130 mL xylene in glove box under nitrogen protection. Fourth, the freshly prepared $Co_2(CO)_8$/xylene solution was injected into the flask to obtain a theoretical 20.0 wt% Co in PP/ MA-g-PP matrix. (Calculation was based on the pure elemental cobalt weight fraction). Keep stirring constant at 200 rpm and heating constant at 140 °C, the solution was immediately turned from transparent to brown and then gradually black during an additional 3-hour refluxing process. The reflux speed was controlled at approximately 1-2 drops/sec in order to maintain a smooth reaction. Finally, the solution was cooled down to room temperature in the flask and then poured onto a large glass container to evaporate solvent in the fume hood overnight. The black powders were collected and dried in a vacuum oven at room temperature overnight. The PP/20.0 wt% Co polymer nanocomposites (PNCs) were synthesized for comparison (8.0 g PP and 5.8 g $Co_2(CO)_8$ were used without any MA-g-PP). The MA-g-PP concentration is 5.0 wt% for all the samples except PP/20.0 wt% Co PNCs. The experimental Co loading in this study was controlled at 20.0 wt% constant.

$Co_2(CO)_8$ underwent a series of decomposition reactions, released carbon monoxide under constant heating in solution. The thermal decomposition of $Co_2(CO)_8$ was complex and normally went through intermediates such as $Co_4(CO)_{12}$ and $Co_6(CO)_{16}$ (black color), and other unstable mononuclear Co carbonyls.[1] After the reaction at ~140 °C for several hours, $Co_2(CO)_8$

was fully decomposed and formed metallic Co NPs.[1] Meanwhile, the Co NPs can be further oxidized to form a Co oxide layer on the metallic Co particle surface.

S1.3. Characterization

Wide-angle X-ray diffraction (WAXD) analysis was carried out with a Bruker AXS D8 Discover diffractometer operating with a Cu Kα radiation source. XRD patterns were recorded at 2θ from 30 to 80°.

Transmission electron microscope (TEM) was used to characterize the particle morphology of the as prepared PP PNCs. The samples were observed in a FEI TECNAI G2 F20 microscope at a working voltage of 200 kV. The samples were prepared from the hot solution of PP PNCs by the end of fabrication process. One droplet of diluted hot solution containing the NPs was dropped on a 400-mesh carbon coated copper grid (Electron Microscopy Sciences). The SAED patterns were taken using a large selected-area aperture and recorded using a Gatan SC1000 ORIUS CCD camera. In case the center beam is strong, a needle was placed in the center to block the beam for half of the exposure time (2 seconds) and then it was immediately removed away from the view area, so that the needle appeared in the pattern which blocked the center strong beam for half of the total exposure time.

For the magnetic measurements, a plastic drinking straw was utilized as the sample holder. A small portion of each specimen, ~5-10 mg, was loaded into the straw. The magnetic moment of the sample was measured in a commercial magnetometer (Quantum Design PPMS system) at room temperature, which is a Faraday-extraction type magnetometer. At each field value, 10 scans were measured and averaged.

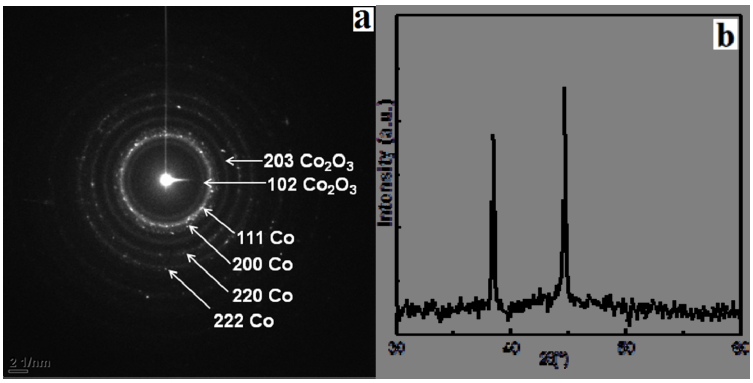

Figure S1. (a) SAED, and (b) XRD pattern of PP/20.0 wt% Co nanocomposites.

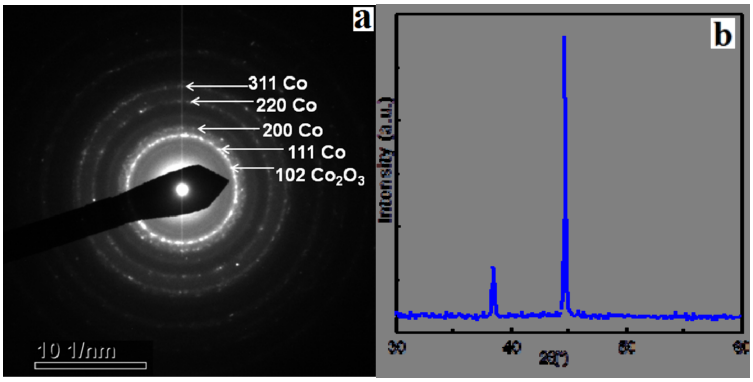

Figure S2. (a) SAED, and (b) XRD pattern of PP/20.0 wt% Co nanocomposites with MA-g-PP (M_n=2500).

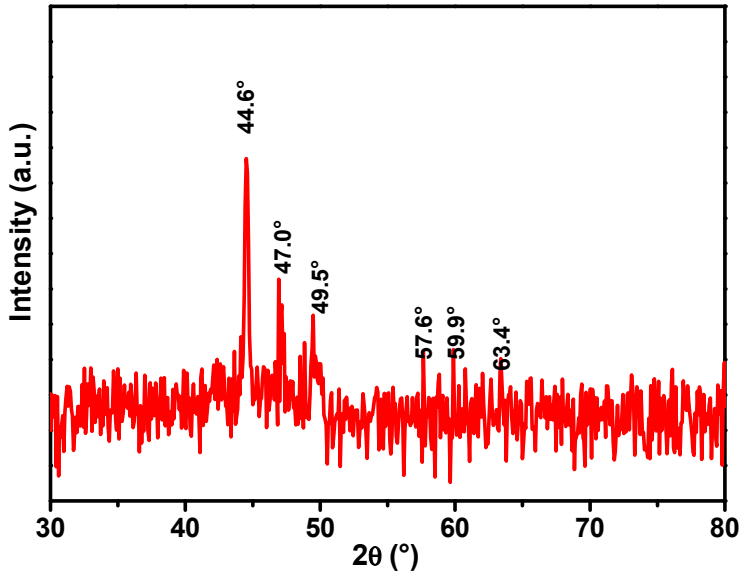

Figure S3. XRD pattern of PP/20.0 wt% Co NPs nanocomposites with MA-g-PP (M_n=800)

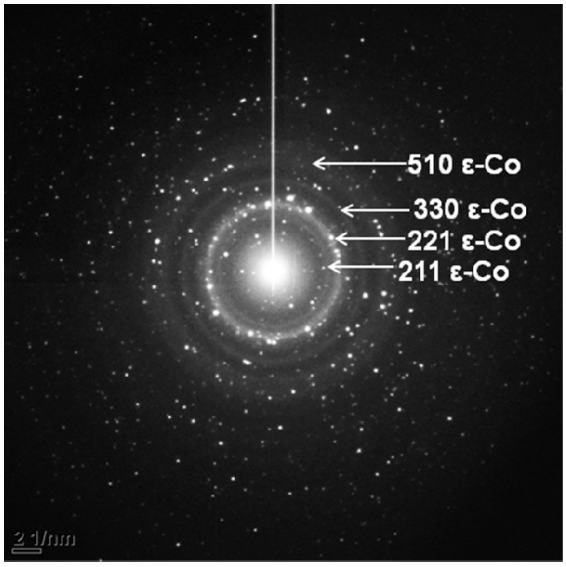

Figure S4. SAED pattern of PP/20.0 wt% Co NPs nanocomposites with MA-g-PP (M_n=800). Lattice spacing of 2.48 Å, 2.02Å, 1.43 Å, and 1.20 Å are corresponding well to those of the (211), (221), (330) and (510) reflection of ε-Co, respectively.[2] The complex spots are primarily due to the cobalt oxide formed on the surface of ε-Co. Due to the sophisticated facets of, the complex oxide formed on these ε-Co nanoparticle surfaces cannot be indexed.

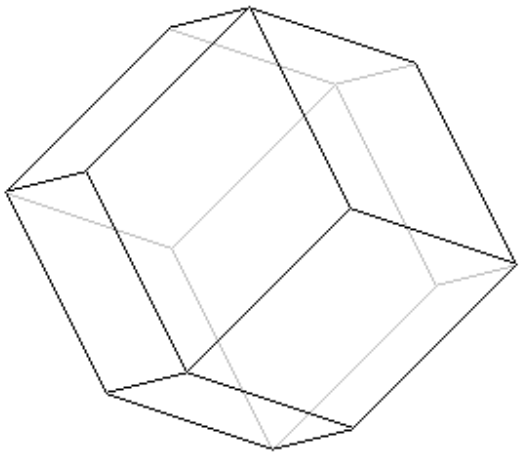

Scheme S2. Rhombic dodecahedron structure of ε- phase cobalt. (More detailed facet information can be reviewed from reference by Z.L. Wang)[3]

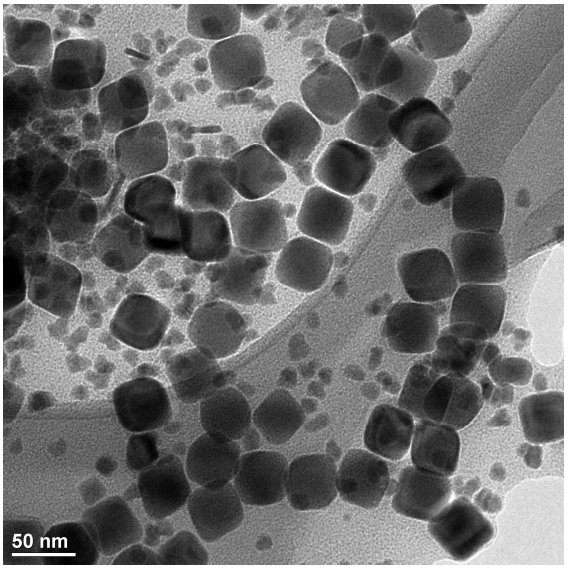

Figure S5. TEM image of PP/20.0 % Co PNCs with 5.0% MA-g-PP (M_n=800).

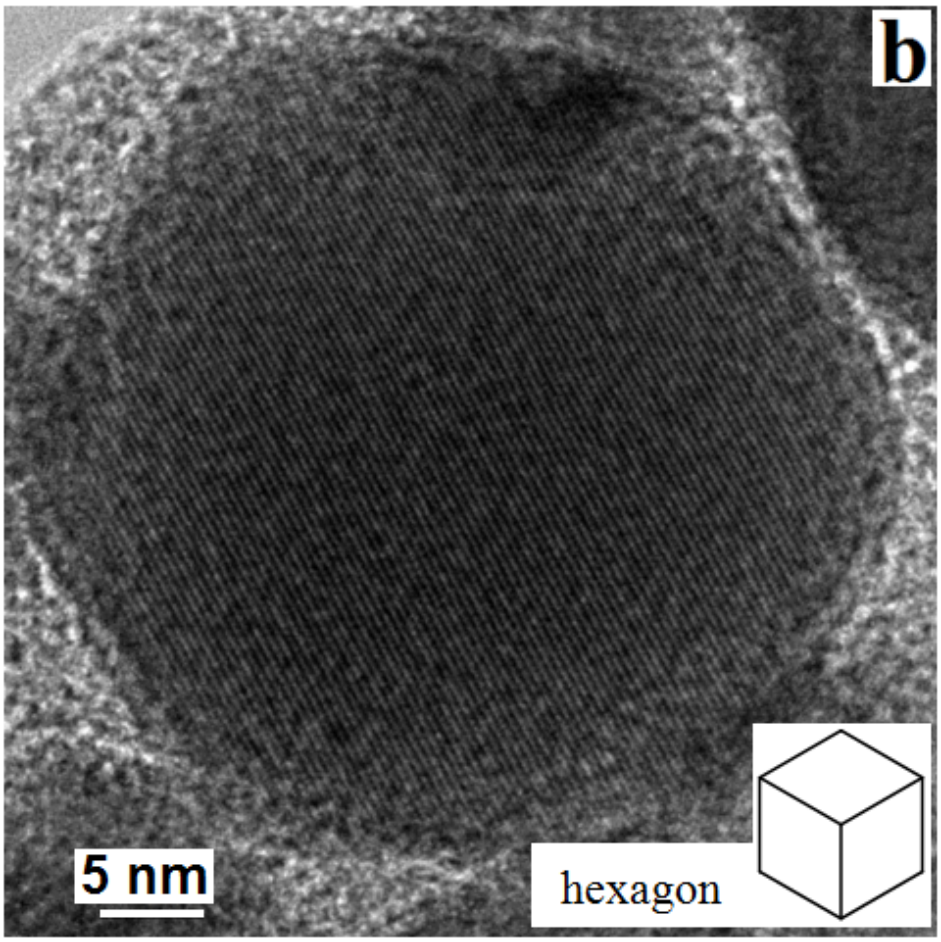

Figure S6. Enlarged HRTEM image of Figure 3b for clear surface coating.

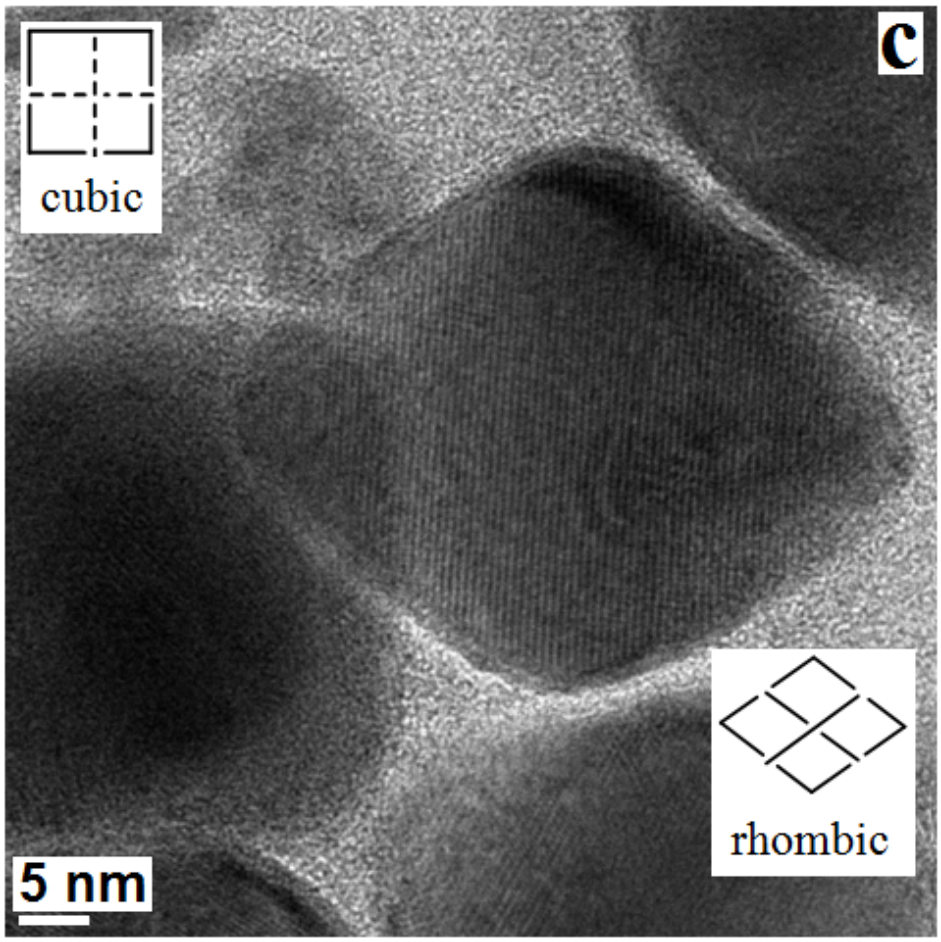

Figure S7. Enlarged HRTEM image of Figure 3c for clear surface coating.

Generally, the solution-based chemical synthesis approach is known to be kinetically, not thermodynamically controlled.[4-6] And different surfactants can effectively control the growth of individual faults which finally manipulate the formation of different crystal phase. For the assembly morphology, it is well known that the use of high boiling solvents allow the slow evaporation at room temperature, which in turn lead to the particle diffusion pathway favor the lowest energy sites during evaporation. The final arrangement of the Co nanocrystal (NC) assembly is controlled by the balance of surface tension, Van der Waals forces, magnetic dipolar-dipolar interactions among these ferromagnetic NCs.[5] Here, xylene has showed the suitability to form the different nanostructure assembly. Due to the strong magnetic dipolar-

dipolar interactions, head-to tail arrangements of individual Co NCs dominated the whole sample assembly to minimize the magnetostatic energy in the presence of weak steric hindrance from the only inert long PP chains. When introducing the long alkyl-chain MA-g-PP, on one hand, the effective passivation of thus prepared Co NCs leads to the formation of more metallic Co, which creates more intense magnetic dipolar-dipolar interactions among individual Co NCs. On the other hand, with the relatively stronger stabilizing effects from long alkyl chain MA-g-PP and steric PP chains among different NCs, the assembly turns out to the coexistence of individual NCs and assembled NC chains. When altering to the short alkyl-chain MA-g-PP, more MA groups were available to form bonding to the same amount of Co nuclei. Thus, the tight coordination of short alkyl chains around the growing NCs is responsible for changing the energetics of growth in favor of the unusual, less dense ε-phase (Figure S5, S6 &S7).[6] Even though the energy difference among α-, β-, and ε- phase Co is small, for example, in α- hcp Co, the sliding of atomic planes often causes Co crystals to display stacking faults.[5] However, it appears that there is no stacking fault in the case of ε- phase Co, which indicates the more energetic cost is needed to slide a crystal structure due to the complicated ε- phase rhombic dodecahedron structure. Hence, the tight bonding of MA-g-PP eventually leads to the metastable ε- phase Co NCs with much larger crystal size. In addition, this stabilizing effect can maintain this ε-phase Co structure more than 9 months by no detectable color change of the resulted powder nanocomposites compared with color changed from black to dark grey for the PP/Co nanocomposites in the absence of MA-g-PP.

Table S1. Magnetic properties of the measured samples.

Samples	M_s (emu/g)	M_s (emu/g) In Pure Co	M_r (emu/g)	H_c (Oe)
PP/Co/ long MA-g-PP	22.8	109.0	7.9	808.0
PP/Co/ short MA-g-PP	25.2	114.0	5.5	242.0
PP/Co	19.5	96.5	7.1	890.0

Reference

1. V. F. Puntes, D. Zanchet, C. K. Erdonmez and A. P. Alivisatos, *Journal of the American Chemical Society*, 2002, **124**, 12874-12880.
2. X. Nie, J. Jiang, E. Meletis, L. Tung and L. Spinu, *Journal of applied physics*, 2003, **93**, 4750-4755.
3. Z. L. Wang, Z. Dai and S. Sun, *Advanced Materials*, 2000, **12**, 1944-1946.
4. S. Sun and C. Murray, *Journal of applied physics*, 1999, **85**, 4325-4330.
5. V. F. Puntes, K. M. Krishnan and A. P. Alivisatos, *Science*, 2001, **291**, 2115-2117.
6. D. P. Dinega and M. G. Bawendi, *Angewandte Chemie International Edition*, 1999, **38**, 1788-1791.